Topology and its Applications 40 (1991) 71-82
North-Holland

Studying links via closed braids II: On a theorem of Bennequin

Joan S. Birman*

Department of Mathematics, Columbia University, New York, NY 10027, USA

William W. Menasco

Department of Mathematics, SUNY at Buffalo, Buffalo, NY 14222, USA

Received 4 April 1989
Revised 23 February 1990

Abstract

Birman, J.S. and W.W. Menasco, Studying links via closed braids II: On a theorem of Bennequin, Topology and its Applications 40 (1991) 71-82.

Links which are closed 3-braids admit very special types of spanning surfaces of maximal Euler characteristic. These surfaces are decribed naturally by words in cyclically symmetric elementary braids which generate the group B_3.

Keywords: Closed braids, links, spanning surfaces for links.

AMS (MOS) Subj. Class.: 57M25.

This paper is the second in a series of papers [2-6] in which the authors have been studying the closed braid representations of links. In this paper we will prove that links which have 3-braid representatives admit very special types of spanning surfaces. Here is one way to describe them. Let $\mathscr{L}$ be an oriented link type of braid index n, in oriented 3-space, and let L be a representative of $\mathscr{L}$. Let F be a (not necessarily connected) oriented spanning surface for L, oriented so that the induced orientation on L is the given one. Then F is a *Bennequin surface* if:

(i) F has maximal Euler characteristic among all such surfaces.

(ii) $L=\partial F$ is a closed n-braid with braid axis A, relative to some choice of a fibration $H=\{H_\theta\colon \theta\in[0,2\pi]\}$ of the open solid torus S^3-A by meridian discs. That is, L meets each H_θ transversally in exactly n points.

(iii) F has a decomposition as a union of n discs, each of which is pierced once by the braid axis A, joined up by half-twisted bands. Also, the singular foliation of F which is induced by its intersections with fibers of H has the properties (see Fig. 1):

(a) each disc is foliated radially;

* Partially supported by National Science Foundation Grant #DMS-88-055672.

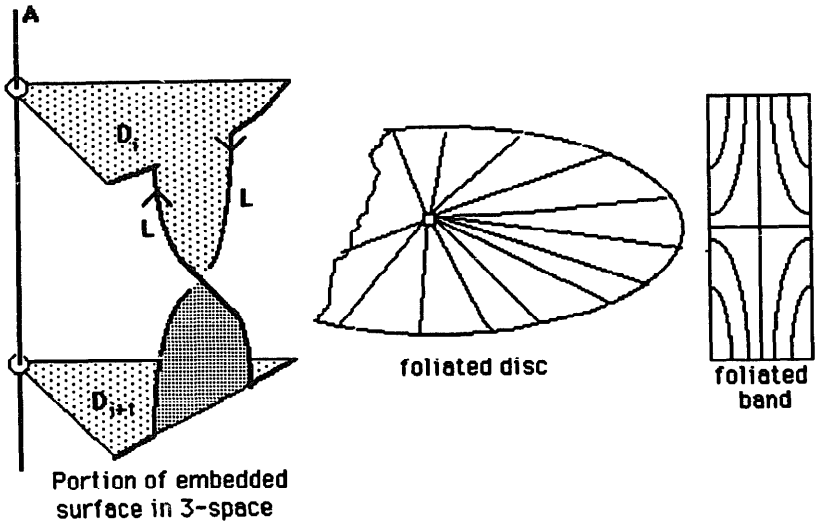

Fig. 1.

(b) each band has a single saddle-point tangency with a fiber of H.

A Bennequin surface and its boundary can be described simultaneously by a single cyclic word $W(L)$ in elementary braids which are associated to the half-twisted bands. Notice that our elementary braids are a little bit different from the usual set of generators of the braid group, in which the strings are lined up in a row and one uses an elementary braid for each crossing between an adjacent pair of strings. For braids which have braid index 3 the new generators are particularly simple: call them a_1, a_2, a_3, where a_i joins the ith disc to the $(i+1)$st (mod 3). They yield a natural braid projection on the surface of a cylinder, and also yield a cyclically symmetric presentation of the 3-strand braid group B_3. The fact that F is a surface of maximum Euler characteristic shows that the cyclic word $W(L)$ is a shortest word in a_1, a_2, a_3.

Bennequin's theorem. *Every link of braid index* ≤ 3 *is the boundary of a Bennequin surface.*

The theorem which we have just stated is a reinterpretation of Proposition 4 of [1]. The main result in this paper will be to give a detailed proof of Bennequin's theorem, which supplements the proof in [1].

There are several reasons why we feel that it is appropriate to take a new look at Bennequin's theorem and its proof at this time. The first is that we need to use it in [4] and the proof in [1] has what appears to us to be a gap at a key point, which will be explained below. Also, Theorem 1 has been assumed by Xu in [9], who has solved the problem of finding, by constructive methods, all Bennequin surfaces which represent a given link type of braid index 3. Her work was motivated by an early version of [4] but actually rested more precisely on the theorem we will prove here. Moreover, the rather simple description we have given of Bennequin

surfaces in terms of discs and bands is natural and useful, however in [1] the surfaces in question were described simply as ones which did not have"poches". Thus one knew that a certain complication did not occur, but lacked a description of the resulting structure which did occur. (See Lemma 3 below.) And, finally, the version of Theorem 1 which we will state and prove below is a little bit stronger than the preliminary version we just gave. The stronger version was necessary in order to fill in the gap in the proof in [1].

To state our version of Bennequin's theorem, we need to describe a special type of spanning surface which was also introduced in [1] and has received some attention (e.g. see [1, 2, 7, 8]). Let $\mathscr{L}$ be an oriented link in oriented 3-space and let L be a representative of $\mathscr{L}$. Let F be a (not necessarily connected) spanning surface for L, oriented so that the induced orentation on L is the given one. Then F is a *Markov surface* if F satisfies properties (i) and (ii) in the definition of a Bennequin surface (however note that n is no longer necessarily the braid index of $\mathscr{L}$), and if property (iii) is replaced by:

(iii)′ There is a singular foliation on F, induced by its intersections with fibers of H, such that:

(a)′ there is a neighborhood on F of each point of $A \cap F$ which is foliated radially;

(b)′ there are only finitely many singular fibers of H, and each has a single saddle-point tangency with F;

(c)′ each nonsingular component c of intersection of F with a fiber H_θ of H is an arc.

Every Bennequin surface is a Markov surface, but there are Markov surfaces which are not Bennequin surfaces. For example, Fig. 2 shows a type of local behavior which can occur in a Markov surface but not in a Bennequin surface.

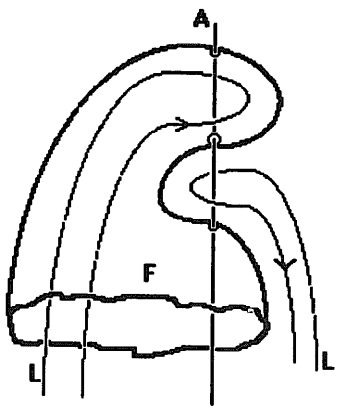

Fig. 2.

By Theorem 4 of [1], or alternatively see Lemma 2 of [2], every spanning surface of maximal Euler characteristic can be modified to a Markov surface. Even more, the modification may be assumed to be by isotopy if $S^3 - \mathscr{L}$ is irreducible.

Let c be a component of $F \cap H_\theta$, where we adopt the convention that H_θ is nonsingular unless it is specifically said to be singular. Thus, by (iii)′ above c is an arc, which then necessarily has its endpoints on $L \cup A$. It is proved in Lemma 1 of [4] that c cannot have both of its endpoints on L. This follows easily from the fact that L is a closed braid. We say that c is an a-*arc*, if one point of ∂c is on L and the other on A and a b-*arc* if both points of ∂c are on A. A b-arc is *essential* if both components of H_θ split along it are pierced by L.

Theorem 1 (cf. [1, Proposition 4]). (i) *Every link of braid index* ≤ 3 *bounds a Bennequin surface.*

(ii) *Assume that* $\mathcal{L}$ *is prime and nonsplit and has braid index* 3. *Let* L *be any* 3*-braid representative of* $\mathcal{L}$. *Let* A *be the braid axis and* H *a fibration of the open solid torus* $S^3 - A$ *by meridian discs. Let* F *be a Markov surface for* L, *relative to fibers of* H. *Assume that all* b*-arcs of intersections of* F *with fibers of* H *are essential. Then* F *is a connected Bennequin surface.*

The beginning of our proof of Theorem 1 is Bennequin's proof of Proposition 4 of [1]. The point of departure occurs at lines 14–17, p. 114 of [1] (and at the point where we refer to figures after 4 in this paper) where Bennequin fails to investigate the end game. If one pursues his argument and investigates the remaining case, one discovers (as we will below) that in fact the surfaces in question are *not* Bennequin surfaces, i.e. they have essential b-arcs, which are Bennequin's "poches". However, on further investigation one sees that the boundaries of these surfaces represent composite link types, and composite links bound *other* surfaces which *are* Bennequin surfaces. Thus the statement of Proposition 4 of [1] is correct, but the proof has a gap.

Proof of Theorem 1. The first part of our proof is a straightforward check that the theorem is true for the cases which are excluded by the hypotheses of (ii). The only link of braid index 1 is the unknot, and it bounds a disc, which is trivially a Bennequin surface. The links of braid index 2 are the 2-component unlink, and the torus links of type $(2, p)$, $p \neq 0, 1$. For each of these the Seifert surface obtained from a 2-braid projection is a Bennequin surface. The split links of braid index 3 are the three-component unlink and the disjoint union of a type $(2, p)$ torus link with the unknot, and again there is an obvious Bennequin surface. Finally, there are the composite links of braid index 3, each of which is the connected sum of torus links of type $(2, p)$ and $(2, q)$. One obtains Bennequin surfaces for these by connect summing the Bennequin surfaces for the summands. Thus we may assume we are in the situation of (ii).

We have a closed 3-braid L which represents a nonsplit prime link of braid index 3, and a Markov surface F with $\partial F = L$. We assume that all b-arcs in $F \cap H_\theta$ are essential. We will show (see Lemma 2 below) that if b-arcs do not occur then F is a Bennequin surface. Our task will then be to prove that b-arcs cannot occur under

the hypotheses of the theorem. This is the situation which is illustrated in the sequence of pictures in Fig. 3. The fibers H_θ are depicted as discs with boundary A. The link L pierces each H_θ three times, transversally. The surface F meets H_θ in three arcs, each having one endpoint on A and the other on L. The arcs in $F \cap H_\theta$ have well-defined sides, which we have labeled + and − to correspond to the + and − sides of F. The axis $A = \partial H_\theta$ is oriented, and by our conventions all three intersections with F are from the − side to the + side. As H_θ is pushed through the fibration H we will encounter a sequence of singular fibers, one of which is illustrated in the third picture in Fig. 3. After the singularity the two arcs which are "surgered" split apart in a new way. Note that the surgery is defined by a "joining arc", indicated as a dotted arc in the first picture. The joining arc necessarily identifies sides of F which have the same parity, because F is orientable. During the complete cycle $\theta \in [0, 2\pi]$ we expect r such surgeries, where r is the number of bands in the disc-band decomposition of F.

We ask how this picture changes when b-arcs are present. A nonsingular fiber H_θ always contains three a-arcs. Each b-arc which is present divides H_θ, and the assumption that all of the b-arcs are essential implies that there is at least one a-arc on each side of the split-apart fiber. The leftmost diagram in Fig. 4 therefore shows the maximum set of b-arcs which can occur. The symbol "w_j" is used to denote $w_j \geq 0$ parallel arcs, $i = 1, 2, 3$. The signs on the a-arcs are determined by the choice of the orientation on A, but the b-arcs could be labeled either way. There are three types of surgery:

type aa: a surgery between two a-arcs,

type ab: a surgery between an a-arc and a b-arc,

type bb: a surgery between two b-arcs.

The set $\{F \cap H_\theta : \theta \in [0, 2\pi]\}$ determines a foliation of F. The fact that the foliation is radial near each of the points where A pierces F implies, immediately: (**) *Every leaf in the foliation is eventually surgered.* Checking the various possibilities for

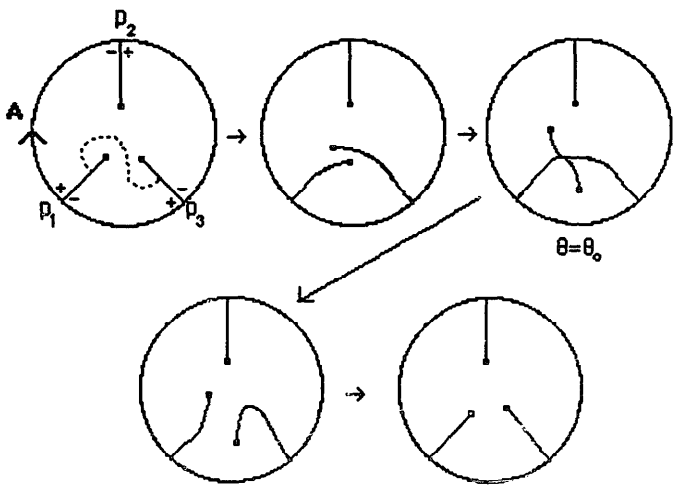

Fig. 3. A sequence of fibers of H showing an F-surgery at $\theta = \theta_0$.

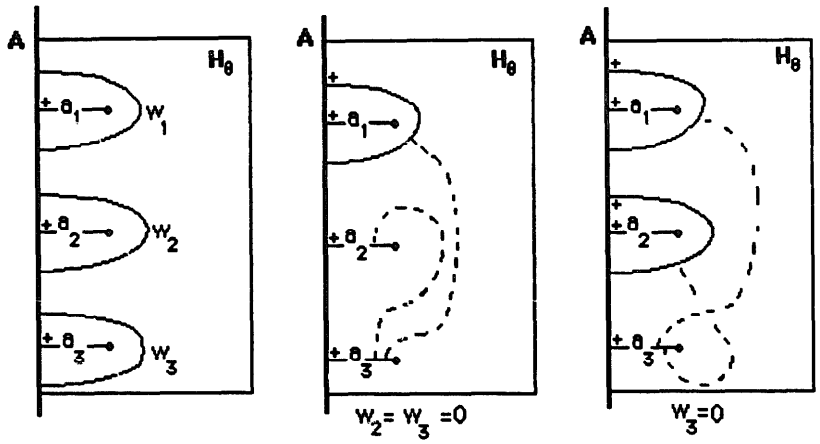

Fig. 4.

surgeries we see immediately that if all three w_i's are nonzero then every possible surgery will produce an inessential b-arc. Thus at least one of the w_i's must be 0. Assume that $w_3 = 0$. Then there are two possibilities.

Case 1. Exactly one of w_1, w_2, w_3 is nonzero, say w_1. See the middle picture in Fig. 4. Then there can either be a unique type aa surgery, after which we will still be in Case 1, or a unique ab surgery, which will bring us to Case 2. These two possible surgeries are indicated by dotted joining arcs.

Case 2. Two of the w_j's, say w_1 and w_2 are nonzero. See the right picture in Fig. 4. There are two possible surgeries, both of type ab, which do not produce inessential b-arcs. The first decreases w_1 by 1 and increases w_2 by 1. The second decreases w_2 by 1 and increases w_1 by 1. Thus if we are in the situation of Case 2, a surgery either keeps us in Case 2 or brings us back to Case 1.

By condition (**) each of the arcs a_1, a_2 and a_3 in Figs. 2 and 3 must experience a surgery as we proceed through the fibration. Even more, the arcs in $F \cap H_\theta$ must return to their initial positions after a variation of 2π in the angle θ. Moreover, the surface F is oriented, so all surgeries must preserve orientations. Assume that initially $k = w_1 \neq 0$, $w_2 = 0$, $w_3 = 0$, as in the middle picture in Fig. 4. Suppose that initially, there are k parallel b-arcs which separate one of the a-arcs from the other two. The first thing that can happen is $p \geq 0$ surgeries of type aa. Then there can be k surgeries of type ab, the net effect of which is to move the entire group of parallel b-arcs. After that, a new sequence of p' unique surgeries of type aa is possible. Then there can be $k' \geq k$ surgeries of type ab which move the group of parallel strands back to their initial position, whence the cycle repeats itself (in general with different p, k, p', k') t times.

In the next lemma we will prove that the cycle of surgeries which we just described determines F as an embedded surface. We will then be able to complete the proof of Theorem 1 by exhibiting an embedded surface F' which realizes the cycle of fibers in Fig. 5. We will see that in the case when $t > 1$ the surface F' does not have maximal Euler characteristic, while in the case $t = 1$ the link L is composite. Thus both cases violate the hypotheses of Theorem 1.

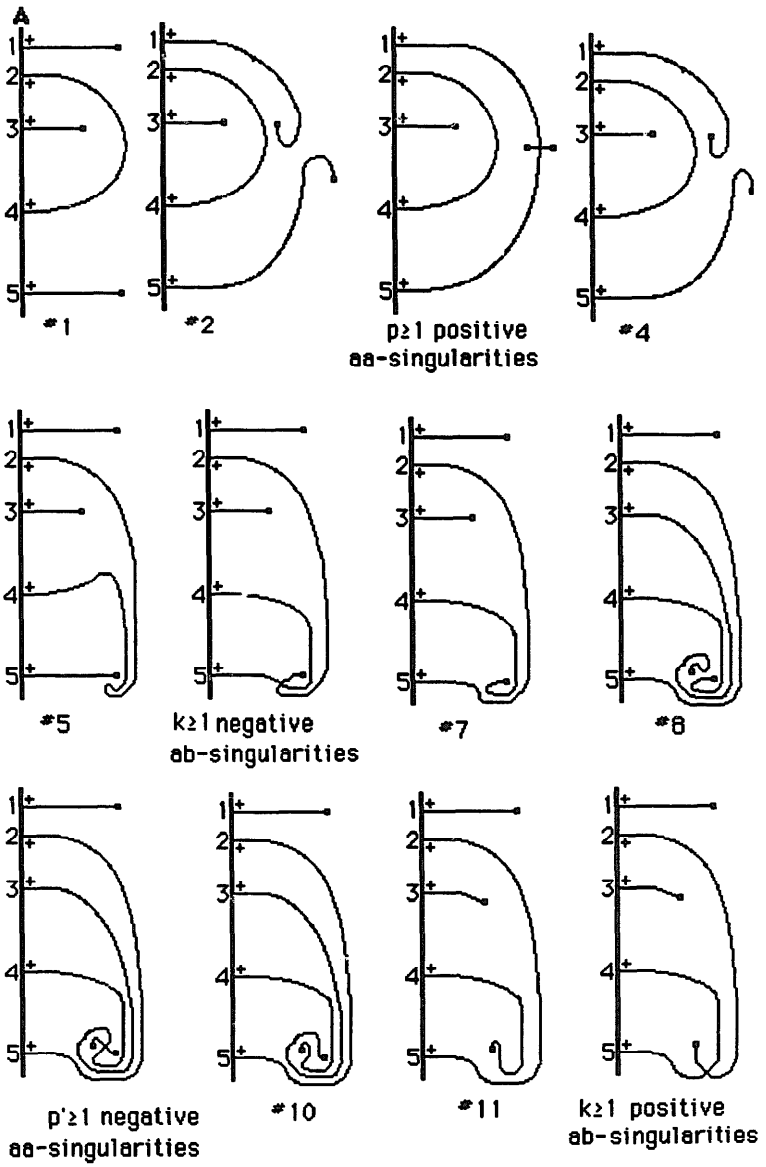

Fig. 5.

The *sign* of a singularity is + or −, according as the outward drawn normal to F points in the direction of increasing or decreasing θ at the singular point. A *cycle of fibers* is the cyclically ordered array of singular fibers, with the components of $F \cap H_\theta$ shown on each H_θ in the cycle.

Lemma 2. *The cycle of fibers determines F as an embedded surface.*

Proof. Suppose that the singularities occur at polar angles $\theta = \theta_1, \theta_2, \ldots, \theta_r$. Each singularity is a saddle-point tangency between F and the fiber in question, and therefore $F \cap H_\theta$, $\theta = \theta_i$, contains a unique pair of singular arcs which intersect at the point of tangency. Figure 6 shows these arcs at typical aa and ab singularities. The points we have labeled $p_i, \ldots$ are on A, and the ones labeled $q_j, \ldots$, are on A

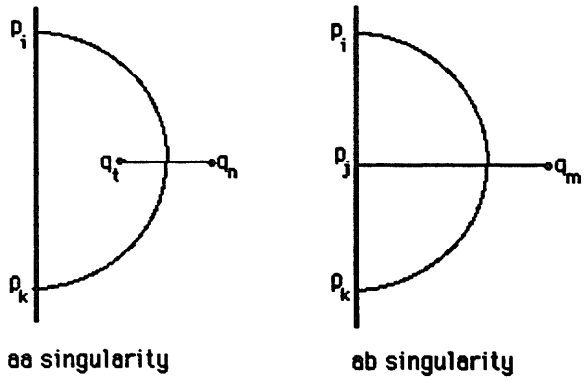

Fig. 6. Singular set, viewed on H_θ.

We pass to 3-space, choosing r fibers and declaring them to be the singular fibers. We then choose an interior point on each singular fiber and declare it to be the singular point, also k points on A which we declare to be $p_1, \ldots, p_k$. Up to homeomorphisms of S^3 which fix A setwise it will not matter how we make these choices. We can then join up the singular points and the p_i's as required to form the singular leaves which end at the p_i's, i.e. on A. The remaining singular leaves which end at the q_j's, on L, can be chosen as arbitrary arcs which end at arbitrary points q_i in the interior of H_θ, subject only to the restriction that the cyclic order on H_θ of the four arcs which meet at the singularity be correct when viewed from the side of H_θ which faces in the direction of increasing θ.

We now extend the embedding of the singular leaves to an embedding of a neighborhood N on F. The two pictures in Fig. 7 show such neighborhoods in the case of aa and ab singularities. They are foliated by the arcs of $F \cap H_\theta$. Since F is transverse to the fibers of H everywhere except along the singular leaves, the only

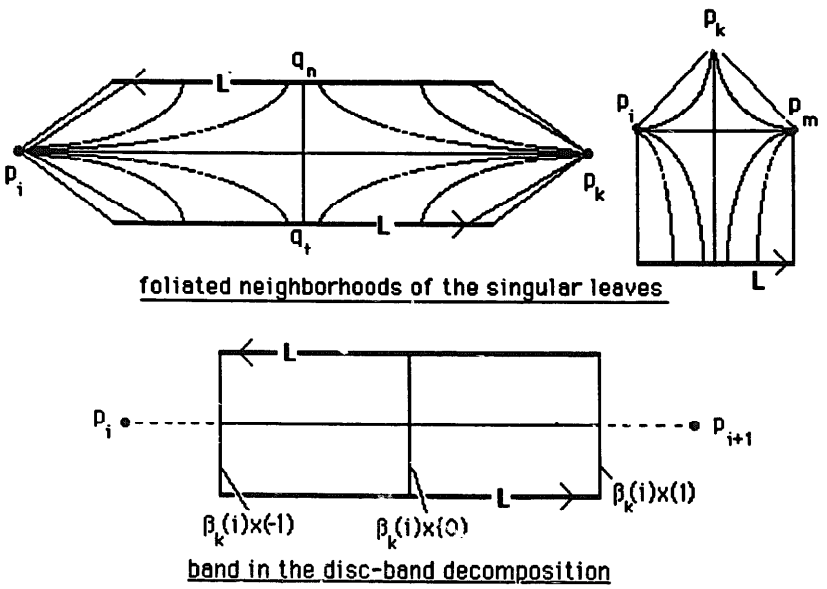

Fig. 7.

problem about how to extend the embedding to N is whether the outward drawn normal to F points in the direction of increasing or decreasing θ, i.e. whether the singularity is positive or negative, and that information is contained in the cycle of fibers.

The complement of the union of all N's on F is a set of discs which are foliated without singularities. This means that they are everywhere transverse to the fibers of H. Thus we can extend the embedding to all of F. This completes the proof of Lemma 2. □

We return to the situation which was under discussion just before the statement of Lemma 2. We had shown that our spanning surface F necessarily determined a cycle of fibers which consisted of $t \geq 1$ rather special subcycles. The ith subcycle consisted of p_i singularities of type aa, followed by k singularities of type ab, then p_i' singularities of type aa, then k of type ab. A typical subcycle was illustrated in Fig. 5. The subcycle begins in #1 with a nonsingular fiber (as in the middle picture in Fig. 4) with three a-arcs and one b-arc (we assume $k=1$). Pictures #2, 3 and 4 in the sequence, which may be repeated p times, illustrate the situation just before, during and after an aa-singularity. The sign is shown as +, but either + or − could occur. Pictures #5, 6 and 7 show a negative ab-singularity. (If $k \geq 1$ the "finger" which is formed by the bb-arc in #5 would be replaced by k nested fingers.) #8, 9 and 10 show an aa-singularity, which may be repeated p' times. The sign is shown as +, but it could be ±, Pictures #11, 12 and 1 show a positive ab-singularity, completing the cycle (if $t=1$).

To construct F' we begin with the case $k=1$. See Fig. 8. Choose five points on the axis A, labeled 1, 2, 3, 4, 5 to correspond to the points on the boundaries of the H_θ's in Fig. 5. Construct horizontal discs D_1, D_3 and D_5 which are pierced by A at their centers, at 1, 3 and 5 respectively, all with their positive sides facing up, and a 2-sphere which is pierced by A at points 2 and 4, and which encloses D_3, with its negative side facing "out". The discs at 1 and 5 are then to be joined up by half-twisted bands, which occur in t groups, the ith group having p_i bands. (Figure 8 shows one of these bands.) The 2-sphere is also joined to D_5, by a tube. (If $t>1$ there will be t tubes.) We need additional bands, more difficult to visualize. The additional bands are to be p' half-twisted bands which join the discs D_3 and D_5, running from D_3 to D_5 inside the tube. (We have shown part of one of the bands.) The band from D_3 passes through the tube, emerging from the underside of D_5, and is folded over before it is attached to D_5, as indicated in the detail. (Compare Fig. 5, #8.) More generally, there will be t tubes, with the ith tube containing a group of p_i bands.

A careful comparison of Fig. 8 with the cycle in Fig. 5 should serve to convince the reader that F' realizes the given cycle of fibers (in the case $k=1$). We now observe that in fact there is a simpler surface, in fact it is a Bennequin surface, with the same boundary—obtained from F' by deleting the 2-sphere and its attaching tubes, filling in the hole in D_5, and then unrolling the bands which join D_3 to D_5

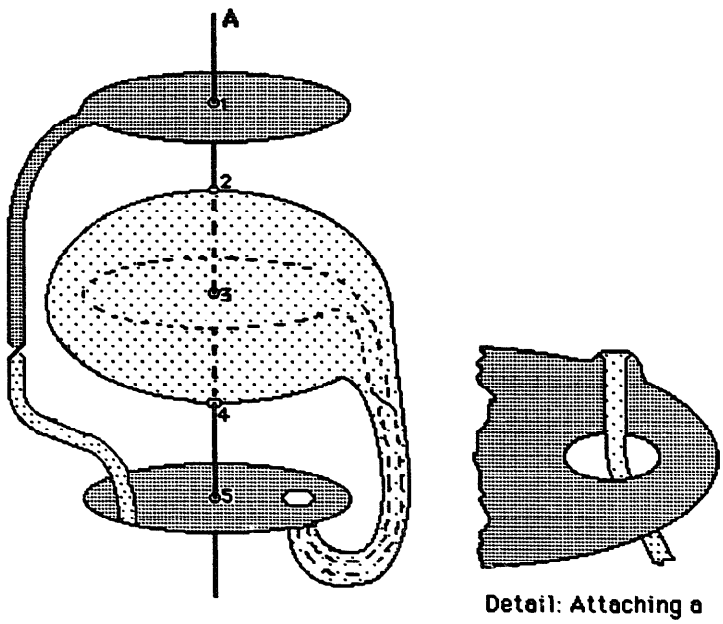

Fig. 8.

to remove the self-intersections which would be created otherwise. Even more, if $t > 1$ this new surface F will have higher Euler characteristic than did F', contradicting our hypothesis about F', because removing the tubes raises the Euler characteristic. This shows that the case $t > 1$, $k = 1$, cannot occur.

We now consider the construction of F' in the case $t \geq 1$, $k > 1$. See Fig. 9, which represents the case $k = 2$ and is to be compared with Fig. 5, #8. There will be three

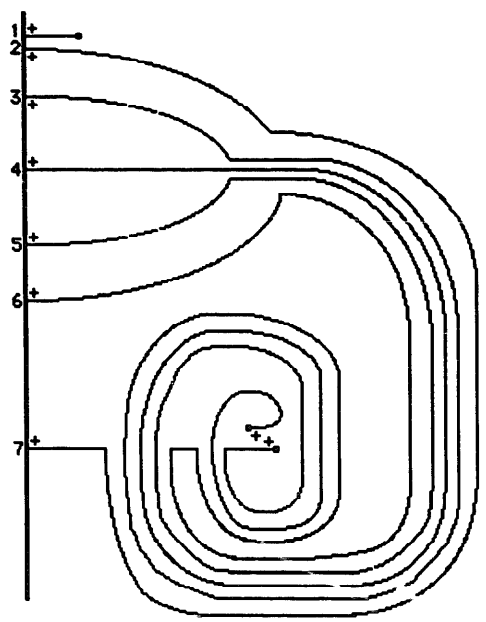

Fig. 9.

discs as before, only now they are numbered D_1, D_{2+k}, D_{3+2k}. The middle disc lies inside k concentric spheres, which are joined up, one at a time, by k (nested) tubes to D_{3+2k}. There are p' bands joining D_{2+k} to D_{3+2k}, one of which is shown in Fig. 9. These bands run through the innermost tube, approach D_{3+2k} from the $-$ side, and then spiral about k times before they are attached. As before, there is a simpler surface with the same boundary. It is the Bennequin surface obtained by removing the k spheres and their attaching tubes, and unwinding the bands. As before, if $t>1$ it has higher Euler characteristic than did F', contrary to hypothesis. The case $t=1$, with arbitrary p, k, p', remains. The tubes can be cut off as before to produce a Bennequin surface, however, we encounter a new difficulty because the Euler characteristic of the Bennequin surface will be the same as that of F'. However, in this case our link is seen to be the connected sum of type $(2, p)$ and type $(2, p')$ torus links, because there are only two blocks of bands, a block of p bands joining one disc pair and a block of p' bands joining the other. This contradicts the hypothesis that L is prime.

The only thing which remains to conclude the proof of Theorem 1 is that F has a disc-band decomposition relative to (A, H).

Lemma 3. *A Markov surface F for a closed n-braid which is foliated without* b*-arcs (or which has no poches, in the language of* [1]*) has a natural decomposition as a union of n horizontal discs joined up by half-twisted bands, one for each* aa*-singularity in the cycle.*

Proof. We prove the result for 3-braids, but it is clearly true in a more general setting. By hypothesis there are no b-arcs in the foliation of F. Therefore the axis A pierces F in exactly three points, p_1, p_2 and p_3, where subscripts are understood to be defined mod 3. We label these points to correspond to their cyclic order on A and study one of the singularities in the foliation of F. It was shown earlier (see the top pictures in Fig. 7) that two singular leaves, which we will refer to as the *α-leaf* and the *β-leaf* pass through the singularity, where $\partial\alpha$ is on the axis A and $\partial\beta$ is on the link L. Thus α joins some p_i to p_{i+1}. Let r_i be the number of type a singular leaves which join p_i to p_{i+1}, so that $r=r_1+r_2+r_3$. These r_i leaves have a natural cyclic order which is determined by the polar angle function, so we can label them $\alpha_i(k)$, $k=1, 2, \ldots, r_i$. Let $\beta_i(k)$ denote the corresponding β-leaf. The collection of all of the β-leaves is thus $\{\beta_i(k)\colon k=1, 2, \ldots, r_i \text{ and } i=1, 2, 3\}$.

We focus on one such $\beta_i(k)$. See the bottom picture in Fig. 7. Let $b_i(k)=\beta_i(k)\times[-1, 1]$ be a product neighborhood of $\beta_i(k)$ on F, the singular leaf being identified with $\beta_i(k)\times\{0\}$. Assume the $b_i(k)$ are chosen to be pairwise disjoint. The $b_i(k)$'s are the bands in our disc-band decomposition of F. Their complement on F is a union of three discs, the ith disc being a neighborhood on F of p_i. The band $b_i(k)$ is attached to D_i along $\beta_i(k)\times\{-1\}$ and to D_{i+1} along $\beta_i(k)\times\{1\}$. The other two edges of the band are on L. Each D_i is joined to D_{i+1} by r_i bands and to D_{i-1} by r_{i-1} bands. The boundary of D_i is a union of the band edges $\beta_i(k)\times\{-1\}$,

$1 \leq k \leq r_i$; the band edges $b_{i-1}(m) \times \{1\}$, $1 \leq m \leq r_{i-1}$, and the segments on L which run between them. This gives our standard disc-band decomposition of F.

Let a_i denote the elementary braid which corresponds to the half-twisted band $b_i(k)$. Since the union of all of the bands is a cyclically ordered set we can associate to L a cyclically ordered word W in the symbols a_1, a_2 and a_3 and their inverses. Two of these symbols, say a_1 and a_2, will be the standard elementary braids which generate B_3. The third symbol a_3 will be a conjugate of a_2 by a_1. This word defines our standard Bennequin surface F of maximal Euler characteristic with boundary L, and also determines L as a closed 3-braid. This completes the proof of Lemma 3, and so also of Theorem 1. □

References

[1] D. Bennequin, Entrelacements et equations de Pfaff, Astérisque 107-108 (1983) 87-161.
[2] J. Birman and W. Menasco, Studying links via closed braids: A finiteness theorems, Preprint.
[3] J. Birman and W. Menasco, Studying links via closed braids III: Classifying links which are closed 3-braids, Preprint.
[4] J. Birman and W. Menasco, Studying links via closed braids: Split links and composite links, Invent. Math. 102 (1) (1990) 115-139.
[5] J. Birman and W. Menasco, Studying links via closed braids V: The unlink, Trans. Amer. Math. Soc., to appear.
[6] J. Birman and W. Menasco, Studying links via closed braids VI: A non-finiteness theorem, Preprint.
[7] A. Douady, Noeuds et structures de contact en dimension 3, Séminaire Bourbaki 604, 35e année, 1982/83.
[8] L. Rudolph, Special positions for surfaces bounded by closed braids, Rev. Mat. Iberoamericana 1 (3) (1985).
[9] P.J. Xu, PhD Thesis, Columbia University, manuscript in preparation.